Available online at www.sciencedirect.com
ScienceDirect
Polyhedron 26 (2007) 4602–4608
POLYHEDRON
www.elsevier.com/locate/poly

Two-stage formation of chloro (*N*-*o*-chlorobenzamido-*meso*-tetraphenylporphyrinato) zinc(II) methylene chloride solvate: Zn(*N*-NHCO(*o*-Cl)C_6H_4-tpp)Cl · CH_2Cl_2

Chun-Yi Chen [a], Hua-Yu Hsieh [a], Jyh-Horung Chen [a,*], Shin-Shin Wang [b], Jo-Yu Tung [c,*], Lian-Pin Hwang [d]

[a] *Department of Chemistry, National Chung Hsing University, Taichung 40227, Taiwan*
[b] *Material Chemical Laboratories ITRI, Hsin-Chu 300, Taiwan*
[c] *Department of Occupational Safety and Health, Chung Hwai University of Medical Technology, Taiwan*
[d] *Department of Chemistry, National Taiwan University and Institute of Atomic and Molecular Sciences, Academia Sinica, Taipei 10764, Taiwan*

Received 11 April 2007; accepted 14 June 2007
Available online 4 July 2007

Abstract

The coordinating properties of *N*-*o*-chlorobenzamido-*meso*-tetraphenylporphyrin (*N*-NHCO(*o*-Cl)C_6H_4-Htpp; **11**) have been investigated for the Zn^{2+} ion. Insertion of Zn results in the formation of the zinc complex Zn(*N*-NCO(*o*-Cl)C_6H_4-tpp)(MeOH) · MeOH (**12** · MeOH). The diamagnetic **12** · MeOH can be transformed into the diamagnetic Zn(*N*-NHCO(*o*-Cl)C_6H_4-tpp)Cl · CH_2Cl_2 (**13** · CH_2Cl_2) in a reaction with aqueous hydrogen chloride (2%). X-ray structures for **12** · MeOH and **13** · CH_2Cl_2 have been determined. The coordination sphere around the Zn^{2+} ion in **12** · MeOH is a distorted trigonal bipyramid with N(2), N(4) and O(2) lying in the equatorial plane, whereas for the Zn^{2+} ion in **13** · CH_2Cl_2, it is a square-based pyramid in which the apical site is occupied by the Cl(1) atom.

Keywords: Zinc; X-ray diffraction; Acid hydrolysis; Two-stage process; *N*-Substituted-*N*-aminoporphyrin

1. Introduction

The absolute values of hardness η for Zn^{2+}, Cd^{2+} and Hg^{2+} are 10.88, 10.29 and 7.7 eV, respectively [1]. The softness of acidity increases from Zn^{2+} to Cd^{2+} to Hg^{2+}. Insertion of $Cd(OAc)_2$ into *N*-NHCO-C_6H_5-Htpp (**1**) [*N*-NHCO-2-C_4H_3O-Htpp (**2**) or *N*-NHCO-2-C_4H_3S-Htpp (**3**)] results in the formation of a six-coordinate diamagnetic complex Cd(*N*-NHCOC_6H_5-tpp)(OAc) (**4**) [Cd(*N*-NHCO-2-C_4H_3O-tpp)(OAc) (**5**) or Cd(*N*-NHCO-2-C_4H_3S-tpp)-(OAc) (**6**)] in 54% (55% or 52%) yield [2,3] (Scheme 1).

Mercury (II) is readily inserted into (**3**) yielding exclusively the four-coordinate diamagnetic complex HgPh-(*N*-NHCO-2-C_4H_3S-tpp) (**7**) in 58% yield [4]. Compounds **4**–**7** are cadmium(II) and mercury(II) complexes of *N*-substituted-*N*-aminoporphyrins. Prompted by these results, we focused on the synthesis of zinc(II) complexes of a similar kind. In addition, the intermediate acid Zn^{2+} attacks the two N–H protons of **1** [or *N*-*p*-$HNCOC_6H_5NO_2$-Htpp (**8**)] and leads to a five-coordinate distorted trigonal bipyramidal Zn(II) derivative Zn (*N*-$NCOC_6H_5$-tpp)(MeOH) (**9**) [or Zn(*N*-*p*-$NCOC_6H_5NO_2$-tpp)(MeOH) (**10**)] possessing a nitrene moiety inserted between the zinc atom and one nitrogen atom, N(4) [2,5]. In **1**, when the *ortho* proton is replaced by a chloro ligand, the new free aminated porphyrin is formed, namely, *N*-*o*-chlorobenzamido-*meso*-tetraphenylporphyrin [*N*-NHCO(*o*-Cl)C_6H_4-Htpp; **11**]. A thorough literature review reveals that there is no report on a metal complex

* Corresponding authors.
E-mail address: JyhHChen@dragon.nchu.edu.tw (J.-H. Chen).

0277-5387/$ - see front matter © 2007 Elsevier Ltd. All rights reserved.
doi:10.1016/j.poly.2007.06.021

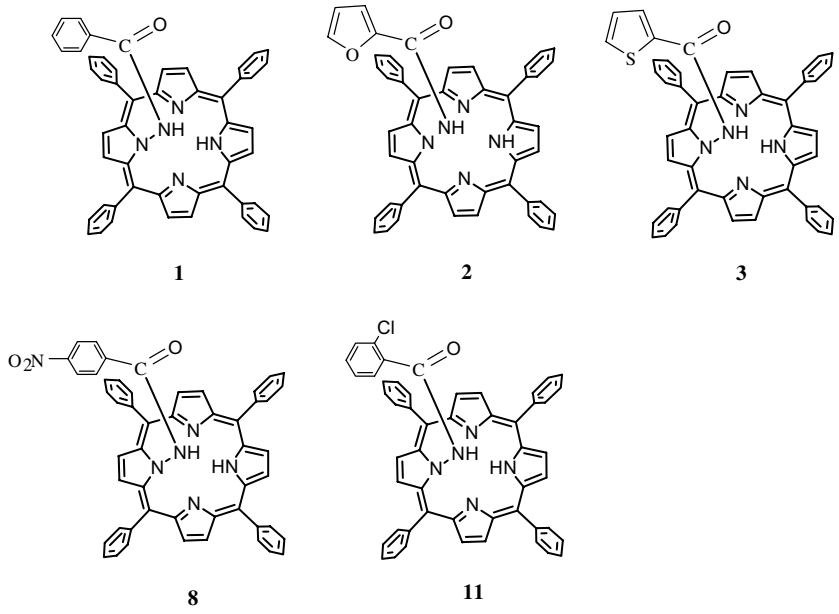

Scheme 1.

of **11**. The lack of study on metal complexes of ligand **11** prompted us to undertake the synthesis and structural investigations of the zinc(II) complexes. Zn(II) is a diamagnetic ion and maintains the d^{10} electron configuration which minimizes intrinsic coordination geometry preferences whilst favoring coordination by ligands of intermediate basicity. In this paper, we describe the X-ray structural investigation on the metallation of **11** leading to the mononuclear zinc(II) complex (*N*-*o*-chlorobenzimido-*meso*-tetraphenylporphyrinato)(methanol)zinc(II) methanol solvate [Zn(*N*-NCO(*o*-Cl)C_6H_4-tpp)(MeOH) · MeOH; **12** · MeOH]. Tsurumaki et al. have reported the electronic structures of oxidized metalloporphyrin complexes by acid-induced cleaveage of Ni(II) complexes of tetraarylporphyrin *N*-oxides at −25 °C [6]. A similar kind of acid hydrolysis was reported by Latos-Grazynski and co-workers for the cleavage of the Ni–O bond in nickel-(II)-6,11,16,21-tetraphenyl-22-hydroxy-*m*-benziporphyrin (TPBPO)Ni^{II}, leading to (TPBPOH)$Ni^{II}Cl$, and for the cleavage of the Ni–C bond in nickel(II)-6,11,16,21-tetraphenyl-*m*-benziporphyrin, leading to chloronickel(II)-22-*H*-6,11,16,21-tetraphenyl-*m*-benziporphyrin [7,8]. We tried to apply acid-hydrolysis to Zn–N bond cleavage in **12** · MeOH. The Zn–N bond in **12** · MeOH is cleaved by addition of aqueous HCl (2%) to a CH_2Cl_2 solution of the complex leading to the desired complex chloro(*N*-*o*-chlorobenzamido-*meso*-tetraphenylporphyrinato)zinc(II) methylene chloride solvate [Zn(*N*-NHCO(*o*-Cl)C_6H_4-tpp)Cl · CH_2Cl_2; **13** · CH_2Cl_2]. Intramolecular hydrogen bonding between the *ortho* chlorine and (*o*-Cl)benzamido hydrogen might enhance the formation of complex **13**. Collectively, we describe the two-stage formation of **13** and the spectroscopic properties of complexes **12** and **13**.

2. Experimental

2.1. *N*-NHCO(*o*-Cl)C_6H_4-Htpp (**11**)

Compound **11** was prepared in 32% yield in the same way as described for *N*-NHCOC_6H_5-Htpp using 2-chlorobenzoyl azide [2]. Compound **11** was dissolved in CH_2Cl_2 and layered with MeOH to give a purple solid. ^{1}H NMR (559.95 MHz, $CDCl_3$, 20 °C) δ: 9.10 [d, 2H, H_β, ^3J(H–H) = 4.2 Hz]; 8.86 [d, 2H, H_β, ^3J(H–H) = 4.8 Hz]; 8.57 [s, 2H, H_β]; 8.15 [s, 2H, H_β]; 8.20 [d, 2H, *ortho* protons *o*-H, ^3J(H–H) = 6.0 Hz]; 8.10 [d, 2H, *o*-H, ^3J(H–H) = 6.6 Hz]; 7.76–7.85 (m, 12H, *meta* and *para* protons); 5.94 [t, 1H, (*o*-Cl)BA-Ph-H_4 (where (*o*-Cl)BA = the *o*-chlorobenzamido ligand), ^3J(H–H) = 7.5 Hz]; 5.70 [d, 1H, (*o*-Cl)BA-Ph-H_3, ^3J(H–H) = 7.8 Hz]; 5.34 [t, 1H, (*o*-Cl)BA-Ph-H_5, ^3J(H–H) = 7.5 Hz]; 2.13 [d, 1H, (*o*-Cl)BA-Ph-H_6, ^3J(H–H) = 7.8 Hz]; −0.26 [bs, 2H, NH]. *Anal.* Calc. for $C_{51}H_{34}ClN_5O$: C, 79.73; H, 4.46; N, 9.12. Found: C, 79.29; H, 4.29; N, 9.05%. MS(FAB): $(M)^+$ 768 (calc. for $C_{51}H_{34}ClN_5O$: 768). UV–Vis spectrum, λ (nm) [$\varepsilon \times 10^{-3}$ (M^{-1} cm^{-1})] in CH_2Cl_2: 429 (213.9), 540 (10.8), 579 (9.7), 637 (7.4). IR (KBr) cm^{-1}: 3052 [ν(CH)], 1624 (amide I band), 1548 (amide II band), 1307 (amide III band), 1594 and 1462 (phenyl ring), 1439 [ν(CN)], 754 [ν(CCl)].

2.2. Zn(*N*-NCO(*o*-Cl)C_6H_4-tpp)(MeOH) · MeOH (**12** · MeOH)

Compound **12** was prepared in 75% yield in the same way as described for Zn(*N*-NCOC_6H_5-tpp)(MeOH) · MeOH using *N*-NHCO(*o*-Cl)C_6H_4-Htpp [2], with a reaction temperature of 30 °C and a reaction time of 30 min.

Compound **12** was dissolved in CH_2Cl_2 and layered with MeOH to obtain purple crystals for single-crystal X-ray analysis. ^{1}H NMR (559.95 MHz, $CDCl_3$, 20 °C) δ: 9.12 [d, 2H, H_β(2,13), ^3J(H–H) = 4.2 Hz]; 8.88 [d, 2H, H_β(3,12), ^3J(H–H) = 4.2 Hz]; 8.78 [s, 2H, H_β(7,8)]; 7.76 [s, 2H, H_β(17,18)]; 8.36 [d, 2H, *ortho* protons *o*-H(26,28), ^3J(H–H) = 7.8 Hz]; 8.09 [d, 2H, *o*-H(22,32), ^3J(H–H) = 6.6 Hz]; 8.84 [bs, 2H, *ortho* protons *o′*-H(38,40)]; 8.21 [bs, 2H, *o′*-H(34,44)]; 7.72–7.87 (m, 12H, *meta* and *para* protons); 6.10 [t, 1H, (*o*-Cl)BA-Ph-H_4, ^3J(H–H) = 7.2 Hz]; 5.91 [d, 1H, (*o*-Cl)BA-Ph-H_3, ^3J(H–H) = 7.8 Hz]; 5.69 [t, 1H, (*o*-Cl)BA-Ph-H_5, ^3J(H–H) = 7.8 Hz]; 3.61 [d, 1H, (*o*-Cl)BA-Ph-H_6, ^3J(H–H) = 7.8 Hz]. *Anal.* Calc. for $C_{53}H_{40}ClN_5O_3Zn$: C, 71.06; H, 4.50; N, 7.82. Found: C, 71.03; H, 4.19; N, 7.47%. MS(FAB): $(M)^+$ 832 (calc. for $C_{51}H_{32}ClN_5OZn$: 832). UV–Vis spectrum, λ (nm) [$\varepsilon \times 10^{-3}$ (M^{-1} cm^{-1})] in CH_2Cl_2: 439 (328.1), 607 (18.8). IR (KBr) cm^{-1}: 3643 [ν(OH)], 3051 [ν(CH)], 1597 (amide I band), 1473 (phenyl and methyl), 1384 (methyl), 1439 [ν(CN)], 753 [ν(CCl)].

2.3. Zn(*N*-NHCO(*o*-Cl)C_6H_4-tpp)Cl · CH_2Cl_2 (**13** · CH_2Cl_2)

Compound **12** (0.06 g, 0.069 mmol) in CH_2Cl_2 (50 ml) was extracted with 2% HCl (50 ml). After the CH_2Cl_2 layer was concentrated to dryness, the residue was redissolved in a minimum of CH_2Cl_2. Removal of the solvent and recrystallization from CH_2Cl_2–CH_3CN [1:1 (v/v)] gave the blue solid **13** (0.059 g, 0.062 mmol, 90%). Compound **13** was dissolved in CH_2Cl_2 and layered with CH_3CN to obtain blue crystals for single-crystal X-ray analysis. ^{1}H NMR (559.95 MHz, $CDCl_3$, 20 °C) δ: 9.03 [d, 2H, H_β(2,13), ^3J(H–H) = 4.8 Hz]; 8.89 [s, 2H, H_β(7, 8)]; 8.89 [d, 2H, H_β(3,12), ^3J(H–H) = 4.2 Hz]; 8.38 [s, 2H, H_β(17,18)]; 8.34 [s, 2H, *ortho* protons *o*-H(26,28)]; 8.12 [s, 2H, *o*-H(22,32)]; 8.77 [s, 2H, *o′*-H(38,40)]; 8.42 [s, 2H, *o′*-H(34,44)]; 7.77–7.94 (m, 12H, *meta* and *para* protons); 6.45 [t, 1H, (*o*-Cl)BA-Ph-H_4, ^3J(H–H) = 7.2 Hz]; 6.23 [t, 1H, (*o*-Cl)BA-Ph-H_5, ^3J(H–H) = 7.8 Hz]; 6.13 [d, 1H, (*o*-Cl)BA-Ph-H_3, ^3J(H–H) = 8.4 Hz]; 5.29 [d, 1H, (*o*-Cl)-BA-Ph-H_6, ^3J(H–H) = 8.1 Hz]; −0.56 [s, 1H, NH]. *Anal.* Calc. for $C_{51}H_{33}Cl_2N_5OZn$: C, 70.56; H, 3.83; N, 8.07. Found: C, 69.99; H, 3.28; N, 8.09%. MS(FAB): $(M - H)^+$ 867 (calc. for $C_{51}H_{33}Cl_2N_5OZn$: 868). UV–Vis spectrum, λ (nm) [$\varepsilon \times 10^{-3}$ (M^{-1} cm^{-1})] in CH_2Cl_2: 440 (306.8), 455 (208.6), 617 (22.2). IR (KBr) cm^{-1}: 3350 [ν(NH)], 3053 [ν(CH)], 1690 (amide I band), 1574 (amide II band), 1274 (amide III band), 1596 and 1480 (phenyl ring), 1441 [ν(CN)], 751 [ν(CCl)].

2.4. Spectroscopy

^{1}H and ^{13}C NMR spectra were recorded at 599.95 and 150.87 MHz, respectively, on Varian Unity Inova-600 spectrometers locked on deuterated solvent, and referenced to the solvent peak. The ^{1}H NMR is relative to $CDCl_3$ at $\delta = 7.24$ and ^{13}C NMR to the center line of $CDCl_3$ at $\delta = 77.0$. HMQC (heteronuclear multiple quantum coherence) was used to correlate protons and carbon through one–bond coupling and HMBC (heteronuclear multiple bond coherence) for two- and three-bond proton–carbon coupling. Nuclear Overhauser effect (NOE) difference spectroscopy was employed to determine the ^{1}H–^{1}H proximity through space over a distance of up to about 4 Å.

The positive-ion fast atom bombardment mass spectrum (FAB MS) was obtained in a nitrobenzyl alcohol (NBA) matrix using a JEOL JMS-SX/SX 102A mass spectrometer. UV–Vis spectra were recorded at 20 °C on a HITACHI U-3210 spectrophotometer. IR spectra were measured at 20 °C in KBr discs on a Bomem, DA8.3 spectrometer. Elemental analyses were obtained using a Heraeus CHN-O-S-Rapid elemental analyzer.

2.5. X-ray crystallography

Table 1 presents the crystal data as well as other information for **12** · MeOH and **13** · CH_2Cl_2. Measurements were taken on a Bruker AXS SMART-1000 diffractometer using monochromatized Mo Kα radiation ($\lambda = 0.71073$ Å) at a temperature of 100(2) K for **12** · MeOH and 297(2) K for **13** · CH_2Cl_2. Empirical absorption corrections were made for both complexes. The structures were solved by direct methods (SHELXL-97) [9] and refined by the full-matrix least-squares method. The (*o*-Cl)BA group within **12** · MeOH is disordered with an occupancy factor of 0.55 for Cl, C(46), C(47), C(48), C(49), C(50), C(51) and

Table 1
Crystal data for **12** · MeOH and **13** · CH_2Cl_2

Compound	**12** · MeOH	**13** · CH_2Cl_2
Empirical formula	$C_{53}H_{40}ClN_5O_3Zn$	$C_{52}H_{35}Cl_4N_5OZn$
Formula weight	895.72	953.02
Space group	$P2_1/n$	$P2_1/c$
Crystal system	monoclinic	monoclinic
a (Å)	14.713(4)	13.8993(16)
b (Å)	16.754(5)	30.995(4)
c (Å)	17.433(5)	11.1975(13)
α (°)	90	90
β (°)	97.933(6)	113.451(2)
γ (°)	90	90
V (Å^3)	4256(2)	4425.5(9)
Z	4	4
F(000)	1856	1952
D_{calc} (g cm^{-3})	1.398	1.430
μ (Mo Kα) (mm^{-1})	0.692	0.843
S	0.961	1.238
Crystal size (mm)	0.25 × 0.15 × 0.10	0.68 × 0.43 × 0.13
θ(°)	28.40	26.02
T (K)	100(2)	297(2)
Number of reflections measured	10496	8684
Number of reflections observed with [$I > 2\sigma(I)$]	7046	6585
R_1^a	0.0610	0.0485
wR_2^b	0.1514	0.1411

[a] $R_1 = [\sum\|\|F_o| - |F_c\|| / \sum|F_o|]$.
[b] $wR_2 = \{\sum[w(F_o^2 - F_c^2)^2] / \sum[w(F_o^2)^2]\}^{1/2}$.

Table 2
Selected bond distances (Å) and angles (°) for compounds **12** · MeOH and **13** · CH_2Cl_2

*Compound **12** · MeOH*			
Bond lengths (Å)			
Zn–N(1)	2.073(3)	Zn–O(2)	2.107(2)
Zn–N(2)	1.944(2)	H(3)···O(1)	1.821(2)
Zn–N(3)	2.067(3)	O(1)···O(3)	2.609(2)
Zn–N(5)	2.013(3)		
Bond angles (°)			
O(2)–Zn–N(1)	88.28(9)	N(1)–Zn–N(2)	94.25(10)
O(2)–Zn–N(2)	111.26(10)	N(1)–Zn–N(3)	169.22(9)
O(2)–Zn–N(3)	95.29(9)	N(1)–Zn–N(5)	84.77(10)
O(2)–Zn–N(5)	117.08(9)	N(2)–Zn–N(3)	95.10(10)
Zn–N(5)–N(4)	95.90(17)	N(2)–Zn–N(5)	131.45(10)
Zn–O(2)–C(52)	131.1(2)	N(3)–Zn–N(5)	85.03(10)
O(3)–H(3)···O(1)	173.65(9)		
*Compound **13** · CH_2Cl_2*			
Bond lengths (Å)			
Zn–N(1)	2.131(2)	Zn–Cl(1)	2.2090(9)
Zn–N(2)	2.007(2)	N(5)···Cl(2)	3.138(2)
Zn–N(3)	2.138(2)	H(5A)···Cl(2)	2.768(2)
Zn···N(4)	2.557(2)		
Bond angles (°)			
Cl(1)–Zn–N(1)	109.81(7)	N(1)–Zn–N(2)	88.65(9)
Cl(1)–Zn–N(2)	120.63(7)	N(1)–Zn–N(3)	136.98(9)
Cl(1)–Zn–N(3)	108.62(7)	N(1)–Zn–N(4)	77.63(9)
Cl(1)–Zn–N(4)	101.04(7)	N(2)–Zn–N(3)	88.05(9)
N(3)–Zn–N(4)	76.78(9)	N(2)–Zn–N(4)	138.30(9)
N(5)–H(5A)···Cl(2)	107.68(9)		

0.45 for Cl′, C(46′), C(47′), C(48′), C(49′), C(50′), C(51′). The phenyl group within **12** · MeOH is disordered with an occupancy factor of 0.5 for C(43), C(44) and 0.5 for C(43′), C(44′). O(1) within **12** · MeOH is disordered with an occupancy factor of 0.9 for O(1) and 0.1 for O(1′). All non–hydrogen atoms were refined with anisotropic thermal parameters, whereas all hydrogen atoms were placed in calculated positions and refined with a riding model. Table 2 lists selected bond distances and angles for complexes **12** · MeOH and **13** · CH_2Cl_2.

3. Results and discussion

3.1. Formation and characterization of *12*

Insertion of $Zn(OAc)_2$ into **11** in a methylene/methanol solution results in the formation of a five-coordinate diamagnetic complex **12** in 75% yield (Scheme 2).

3.2. Crystal structure of *12* · *MeOH*

The structure of **12** · MeOH, determined in an X-ray diffraction study, is shown in Fig. 1a. The geometry around Zn in **12** · MeOH is described as a distorted trigonal bipyramid with N(2), N(5) and O(2) lying in the equatorial plane. The Zn–O(2) bond distance is 2.107(2) Å and the mean Zn-4N distance is 2.024(3) Å for **12** · MeOH. The Zn–O(2) (MeOH) distance of 2.107(2) Å is slightly longer than the sum of the covalent radii of Zn and O (1.92 Å) but is significantly shorter than the sum of the van der Waals radii of Zn and O (2.90 Å) [10]. This Zn–O(2) contact may be described as a weak covalent bond. The distortion in five-coordinate complexes can be quantified by the "degree of trigonality" which is defined as $\tau = (\beta - \alpha)/60$, where "$\beta$" is the largest and "$\alpha$" the second largest of the L_{basal}–M–L_{basal} angles [11]. In **12**, we find $\beta = 169.22(9)°$ [N(3)–Zn–N(1)] and $\alpha = 131.45(10)°$ [N(2)–Zn–N(5)] for **12** · MeOH (Table 2) and thus a τ value of 0.63 is obtained for **12** · MeOH. Hence, the geometry around Zn(II) in **12** · MeOH is best described as a distorted trigonal bipyramid. In **12** · MeOH (Fig. 1a), the observed H(3)···O(1) and O(3)···O(1) distances are 1.821(2) and 2.609(2) Å (Table 2), respectively, which fall below those values expected from van der Waals distances (2.60 and 2.80 Å, respectively). The O(3)–H(3)–O(1) angle is 173.65(9)°, and its deviation from linearity is small. Therefore, this intermolecular hydrogen bonding causes an increased polarization of the carbonyl bond in **12** · MeOH. Consequently, the carbonyl carbon C(45) in **12** · MeOH becomes more positive, thereby accounting for its NMR downfield shift of 2.8 ppm observed at 20 °C, i.e. from 161.5 ppm for C(45) in **13** to 164.3 ppm for the same carbonyl carbon in **12** · MeOH (Tables S1 and S2).

3.3. Formation and characterization of *13*

When a solution of **12** in CH_2Cl_2 is treated with aqueous hydrogen chloride (2%), a new species is formed that can be formulated as **13** (Scheme 2). The reaction is reversed by heating the products in CH_2Cl_2/MeOH at 30 °C for 10 min (Scheme 2).

3.4. Crystal structure of *13* · CH_2Cl_2

The structure of **13** · CH_2Cl_2, determined by an X-ray diffraction study, is shown in Fig. 1b. The (*o*-Cl)BA group lies on the side opposite to the chloride Cl(1) in **13** · CH_2Cl_2. The coordination bond lengths Zn–N(1) 2.131(2) Å, Zn–N(2) 2.007(2) Å, Zn–N(3) 2.138(2) Å and Zn–Cl(1) 2.090(9) Å are within the limit found for zinc(II) porphyrins. The (*o*-Cl)BA nitrogen N(5) in **13** · CH_2Cl_2 is no longer bonded to zinc as indicated by its longer internuclear distance, 2.935(2) Å for Zn···N(5). Moreover, the Zn···N(4) distance of 2.557(2) Å for **13** · CH_2Cl_2 is longer than 2.138(2) Å for Zn–N(3) but is significantly shorter than the sum of the van der Waals radii of Zn and N (2.95 Å) [10]. This longer Zn···N(4) contact in **13** · CH_2Cl_2 may be viewed as a secondary intramolecular interaction. This kind of secondary interaction was earlier observed for Zn(*N*-Me-tpp)Cl with Zn···N1 = 2.530(7) Å [12,13]. Most chemists seem to consider this secondary interaction between the metal ion and the fourth N as a weak bond in *N*-substituted porphyrin metal complexes. In the present case, we find $\beta = 138.30(9)°$ [N(2)–Zn–N(4)] and $\alpha = 136.98(9)°$ [N(1)–Zn–N(3)] for **13** · CH_2Cl_2 and thus a τ value of 0.02 is obtained for **13** · CH_2Cl_2. Hence, the

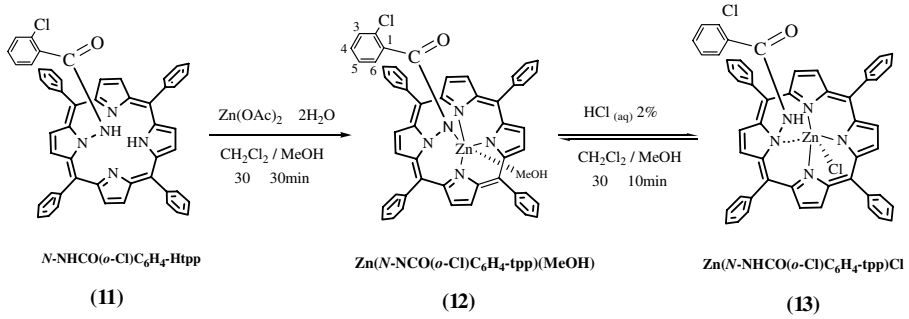

N-NHCO(*o*-Cl)C_6H_4-Htpp (**11**)

Zn(*N*-NCO(*o*-Cl)C_6H_4-tpp)(MeOH) (**12**)

Zn(*N*-NHCO(*o*-Cl)C_6H_4-tpp)Cl (**13**)

Scheme 2.

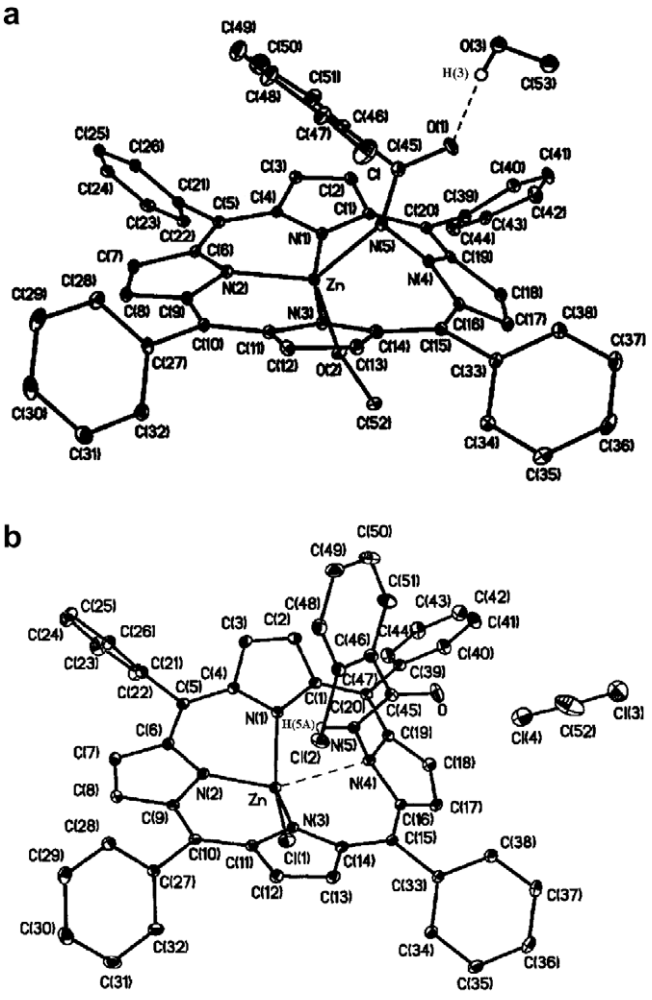

Fig. 1. Molecular configuration and atom-labelling scheme for (a) **12** · MeOH and (b) **13** · CH_2Cl_2, with ellipsoids drawn at 30% probability for both complexes. Hydrogen atoms except H(3) in **12** · MeOH and H(5A) in **13** · CH_2Cl_2 are omitted for clarity.

geometry around Zn(II) in **13** · CH_2Cl_2 is best described as a square-based pyramid with Cl(1) as the apical atom. The τ value of 0.02 obtained for **13** · CH_2Cl_2 is quite close to the value of 0.05 for Zn(*N*-Me-tpp)Cl [12,13]. Hence compounds **13** · CH_2Cl_2 and Zn(*N*-Me-tpp)Cl have a similar coordination geometry around the Zn^{2+} ion. We adopt the plane of three strongly bound pyrrole nitrogen atoms [i.e. N(1), N(2) and N(3)] as a reference plane 3N for **12** · MeOH and **13** · CH_2Cl_2. The zinc ion in **13** · CH_2Cl_2 (or **12** · MeOH) is displaced from the 3N plane by 0.75 Å (or 0.09 Å) toward the chloride [Cl(1)] [or O(2)(MeOH)] (Fig. S1). The occurrence of weak intramolecular hydrogen bonding between the (*o*-Cl)benzamido hydrogen [H(5A)] and the chlorine Cl(2) in **13** is reflected in the long N(5)–H(5A)···Cl(2) bond distance of 2.768(2) Å and acute N(5)–H(5A)···Cl(2) angle of 107.68(9)° (Table 2). This weak intramolecular hydrogen bonding might strengthen the formation of complex **13**.

3.5. ^1H NMR spectroscopy data of 12 and 13 in $CDCl_3$

In solution, the molecule has an effective C_s symmetry with a mirror plane running through the N(2)–Zn–N(5)–N(4) unit for **12** or the N(2)–Zn–N(4)–N(5) unit for **13**. As a result, the ^1H NMR spectra will exhibit four pyrrole resonances [H_β(7,8), H_β(17,18), H_β(3,12), H_β(2,13)] for these two complexes (Fig. 2). Non-equivalence of the two sides of the macrocycle will cause each phenyl ring to have two distinct *ortho* resonances with one set of *ortho* protons, *o*-H(22,32) and *o*-H(26,28), for phenyl C(24) and C(30) and the other set of *ortho* protons, *o′*-H(34,42) and *o′*-H(38,40), for phenyl C(36) and C(42), unless the rotation around the C_{meso}–C_1 [C(5)–C(21), C(10)–C(27) or C(15)–C(33), C(20)–C(39)] bond is sufficiently fast in these two complexes (Fig. 2).

The tautomerism exchange between the two NH protons of **11** in CD_2Cl_2 is fast on the ^1H NMR timescale at both 20 and −90 °C. Hence only one type of N–H proton signal was observed for **11** in CD_2Cl_2 at 20 and −90 °C. At −90 °C, traces of water were frozen from the solution of **11** and **13** in CD_2Cl_2. Thus, the frozen water inhibits intermolecular proton exchange between water and NH protons of **11** and **13**, and allows the observation of a broad singlet for the NH proton at $\delta = -0.51$ ppm ($\Delta\nu_{1/2} = 11.8$ Hz) for **11** and $\delta = -0.69$ ppm ($\Delta\nu_{1/2} = 9.1$ Hz) for **13** at −90 °C. In this case, the NH proton signal for **11** and **13** at −90 °C is broadened by the quadrupolar interaction of the ^{14}N nucleus. The signal arising from the NH proton of **11** in CD_2Cl_2 was observed as a broad singlet at $\delta = -0.29$ ppm ($\Delta\nu_{1/2} = 23$ Hz) at 20 °C. These NMR data suggest that the NH protons of **11** undergo intermediate intermolecular proton exchange with water at 20 °C.

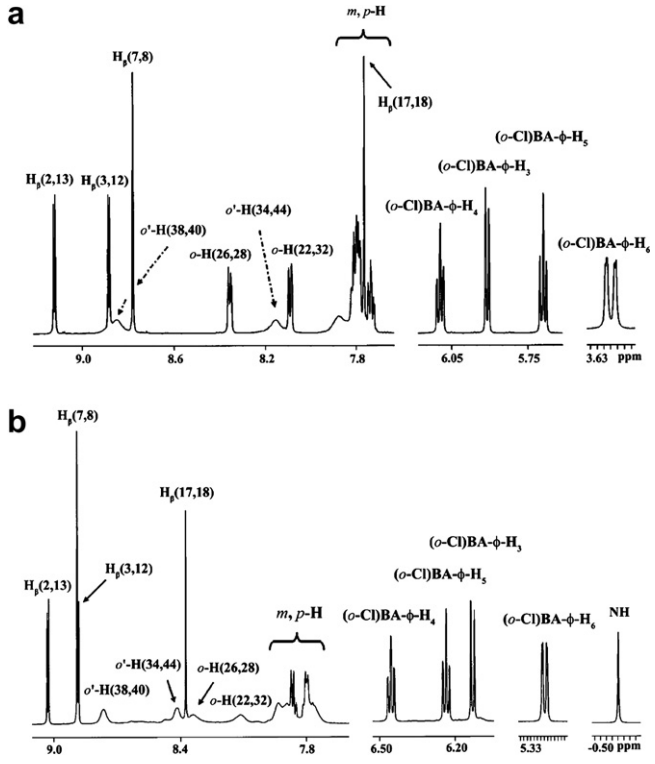

Fig. 2. The 599.95 MHz ^{1}H NMR spectra in $CDCl_3$ at 20 °C for (a) **12** and (b) **13**, where ϕ = Ph (phenyl group).

Moreover, the ^{1}H NMR spectrum of **13** in CD_2Cl_2 showed a sharp singlet at $\delta = -0.58$ ppm ($\Delta\nu_{1/2} = 2.1$ Hz) for the NH proton at 20 °C (see a similar spectrum shown in Fig. 2b). This sharp signal ($\Delta\nu_{1/2} = 2.1$ Hz) is not in agreement with that of $\Delta\nu_{1/2} = 9.1$ Hz found for **13** in the absence of any exchange. Hence, these NMR data for **13** indicate that the NH proton [i.e., H(5A)] bound to N(5) undergoes rapid intermolecular proton exchange with water at 20 °C. Due to the ring current effect, upfield shifts for the ^{1}H resonances of (*o*-Cl)BA-Ph-H_6, (*o*-Cl)BA-Ph-H_3, (*o*-Cl)BA-Ph-H_5 and (*o*-Cl)BA-Ph-H_4 for **13** in $CDCl_3$ at 20 °C are $\Delta\delta = -2.48$ [from 7.77 (obtained from *o*-chlorobenzamide) to 5.29 ppm], −1.29 (from 7.42 to 6.13 ppm), −1.12 (from 7.35 to 6.23 ppm) and −0.95 (from 7.40 to 6.45 ppm), respectively (Fig. 2b). As the distance between the geometrical center (C_t) of the 4N plane and axial protons gets smaller qualitatively, the shielding effect becomes larger [14]. In **13**, the distance for $C_t\cdots$(*o*-Cl)BA-Ph-H_6, $C_t\cdots$(*o*-Cl)BA-Ph-H_3, $C_t\cdots$(*o*-Cl)BA-Ph-H_5 and $C_t\cdots$(*o*-Cl)-BA-Ph-H_4, increases from 5.615, 6.119, 7.138 to 7.312 Å. As the (*o*-Cl)BA-Ph-H_6 proton of **13** is closer to C_t, the shielding gets larger for this (*o*-Cl)BA-Ph-H_6 proton. A similar ring current effect is also observed for **12**. The average distance between $C_t\cdots$(*o*-Cl)BA-Ph-H_6, $C_t\cdots$(*o*-Cl)-BA-Ph-H_5, $C_t\cdots$(*o*-Cl)BA-Ph-H_3 and $C_t\cdots$(*o*-Cl)BA-Ph-H_4 for **12** increases from 3.934, 5.438, 5.684 to 6.166 Å. The fact that all four distances between C_t and (*o*-Cl)BA-Ph protons in **12** are shorter than those distances in **13** indicates that the ring current effect of (*o*-Cl)BA protons in **12** would be larger and in turn the ^{1}H upfield shifts for those protons in the same compound would be still higher. This observation is corroborated by the doublet at 3.61 ppm for (*o*-Cl)BA-Ph-H_6 in **12** and the doublet at 5.29 ppm for the same Ph-H_6 proton in **13**, the triplet at 5.69 ppm for (*o*-Cl)BA-Ph-H_5 in **12** and the triplet at 6.23 ppm for the same Ph-H_5 proton in **13**, the doublet at 5.91 ppm for (*o*-Cl)BA-Ph-H_3 in **12** and the doublet at 6.13 ppm for the same Ph-H_3 proton in **13**, the triplet at 6.10 ppm for (*o*-Cl)BA-Ph-H_4 in **12** and the triplet at 6.45 ppm for the same Ph-H_4 proton in **13** (Fig. 2).

3.6. Solid state IR spectroscopy data of 11, 12 and 13

Compound **12** could be viewed as a tertiary amide and it displayed a unique amide I band at 1597 cm^{-1} in the IR spectrum in the solid state. The two interactions due to a strong intermolecular hydrogen bond between O(1) and H(3) and the covalent bond Zn–N(5) reduces the C=O stretching frequency by 53 cm^{-1} from 1650 cm^{-1} for tertiary amides to 1597 cm^{-1} for **12** [15]. The O–H stretching and methyl bending bands of MeOH in **12** occur near 3643 and 1384 cm^{-1}, respectively. Moreover, compounds **11** and **13** are classified as secondary amides with bands at 1624, 1548 and 1307 cm^{-1} (or 1690, 1574 and 1274 cm^{-1}) being assigned as amide I, II and III bands of **11** (or **13**). These data are quite close to those frequencies of 1680–1630, 1570–1515 and 1300 cm^{-1} reported for amide I, II and III bands of secondary amides [15,16]. The band at 3350 cm^{-1} results from the N(5)–H(5A) stretch of **13**.

4. Conclusion

Two distinct types of zinc complexes, hitherto unreported, have been obtained from *N*-*o*-chlorobenzamido-*meso*-tetraphenylporphyrin (*N*-NHCO(*o*-Cl)C_6H_4-Htpp; **11**). In Zn(*N*-NCO(*o*-Cl)C_6H_4-tpp)(MeOH) (**12**), the N–H bond of the *o*-chlorobenzamido ligand is cleaved and the *o*-chlorobenzamido nitrogen participates in bonding to the zinc ion. In Zn(*N*-NHCO(*o*-Cl)C_6H_4-tpp)Cl (**13**), the *o*-chlorobenzamido [(*o*-Cl)BA] substituent is left intact and the zinc(II) ion is coordinated to the three nitrogens of the macrocycle core. Compound **13** can be synthesized in the reaction of **12** with aqueous HCl (2%).

Acknowledgements

The financial support from the National Science Council of the ROC under Grant NSC 95-2113-M-005-014-MY3 and NSC 95-2113-M-273-002 is gratefully acknowledged.

Appendix A. Supplementary material

CCDC 642339 and 642340 contain the supplementary crystallographic data for **12** · MeOH and **13** · CH_2Cl_2. These data can be obtained free of charge via http://www.ccdc.cam.ac.uk/conts/retrieving.html, or from the Cambridge Crystallographic Data Centre, 12 Union Road,

Cambridge CB2 1EZ, UK; fax: (+44) 1223-336-033; or e-mail: deposit@ccdc.cam.ac.uk. Fig. S1 shows the diagram of the porphyrinato ($C_{20}N_4$, Zn, (*o*-Cl)BA, O(MeOH), Cl) unit of **12** · MeOH and **13** · CH_2Cl_2. Tables S1 and S2 show the ^{13}C NMR (150.87 MHz) for **12** and **13** in $CDCl_3$ at 20 °C. Supplementary data associated with this article can be found, in the online version, at doi:10.1016/j.poly.2007.06.021.

References

[1] R.G. Pearson, Inorg. Chem. 27 (1988) 734.
[2] F.A. Yang, J.H. Chen, H.Y. Hsieh, S. Elango, L.P. Hwang, Inorg. Chem. 42 (2003) 4603.
[3] J.Y. Tung, J.H. Chen, Polyhedron 26 (2007) 589.
[4] H.Y. Hsieh, C.W. Cheng, F.A. Yang, J.H. Chen, J.Y. Tung, S.S. Wang, Personal communication.
[5] C.H. Chen, Y.Y. Lee, B.C. Liau, S. Elango, J.H. Chen, H.Y. Hsieh, F.L. Liao, S.L. Wang, L.P. Hwang, J. Chem. Soc., Dalton Trans. (2002) 3001.
[6] H. Tsurumaki, Y. Watanabe, I. Morishima, Inorg. Chem. 33 (1994) 4186.
[7] M. Stepien, L. Latos-Grazynski, Inorg. Chem. 42 (2003) 6183.
[8] M. Stepien, L. Latos-Grazynski, L. Szterenberg, J. Panek, Z. Latajka, J. Am. Chem. Soc. 126 (2004) 4566.
[9] G.M. Sheldrick, SHELXL-97: Program for the Refinement of Crystal Structure from Diffraction Data, University of Göttingen, Göttingen, Germany, 1997.
[10] J.E. Huheey, E.A. Keiter, R.L. Keiter, Inorganic Chemistry, 4th ed., Harper Collins College Publishers, New York, 1993, pp. 117, 292.
[11] A.W. Addison, T.N. Rao, J. Reedijk, J.V. Rijn, G.C. Verschoor, J. Chem. Soc., Dalton Trans. (1984) 1349.
[12] D.K. Lavallee, A.B. Kopelove, O.P. Anderson, J. Am. Chem. Soc. 100 (1978) 3025.
[13] C.K. Schauer, O.P. Anderson, D.K. Lavallee, J.P. Battioni, D. Mansuy, J. Am. Chem. Soc. 109 (1987) 3922.
[14] C.E. Johnson Jr., F.A. Bovey, J. Chem. Phys. 29 (1958) 1012.
[15] K. Nakanishi, P.H. Solomon, Infrared Absorption Spectroscopy – Practical, 2nd ed., Holden Day, San Francisco, 1977, p. 42.
[16] R.M. Silverstein, F.X. Webster, Spectrometric Identification of Organic Compounds, 6th ed., Wiley, New York, 1998, pp. 99, 101.